NeuroImage 321 (2025) 121521

Contents lists available at ScienceDirect

NeuroImage

journal homepage: www.elsevier.com/locate/ynimg

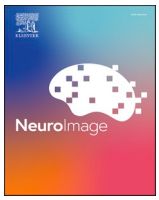

# Brain-wide patterns of oscillatory amplitudes represent naturalistic behavior

Duho Sihn, Sung-Phil Kim *

*Department of Biomedical Engineering, Ulsan National Institute of Science and Technology, Ulsan 44919, Republic of Korea*

ARTICLE INFO

*Keywords:*
Brain-wide distribution
EEG
Naturalistic behavior
Oscillatory amplitude
Traveling wave
Local phase gradient

ABSTRACT

Recent findings indicate that neural representations of behaviors are distributed throughout the brain. These distributed neural representations are likely to accompany the transmission of behavioral information across large-scale brain regions, often mediated by the propagation of brain oscillations. Yet, it remains unknown whether the brain-wide patterns of oscillatory amplitude can represent more naturalistic behaviors, and whether they are related to the brain-wide patterns of oscillatory propagation. Using an open human electroencephalogram (EEG) dataset recorded during video-game play (behaviors: shooting, collecting, crashing), we introduced activation states, momentary brain-wide patterns derived from oscillatory amplitude envelopes. The results showed that brain-wide patterns of activation states reliably predicted the likelihood of each behavior during gameplay, and cross-validated decoding recovered behavioral occurrence from single-trial brain-wide activation patterns. We then quantified large-scale oscillation propagation using the temporal consistency of propagation directionality. We found that the spatial patterns of propagation consistency were strongly correlated with concurrent brain-wide patterns of activation states, indicating that where oscillation amplitudes spatially organize, propagation organizes similarly across the whole brain. Together this study shows novel findings that (1) distributed EEG amplitude patterns are predictive enough to decode naturalistic behavior and (2) large-scale propagation provides a complementary signature that tracks the same brain-wide organization. From these results, we propose a Dual-State Oscillation Model (DSOM) engaging coupled brain-wide activation states (amplitude organization) and propagation states (directional transmission), which may provide a novel framework for linking distributed neural representations to large-scale communication dynamics to elucidate how brain networks coordinate naturalistic behaviors.

## 1. Introduction

Accumulating evidence in neuroscience research indicates that neural representations of various behaviors span widespread regions of the brain (Kaplan and Zimmer, 2020; Westlin et al., 2023). For instance, neural representations of various cognitive functions, such as perception, movement, decision-making, and working memory, are each distributed across large-scale brain areas (Stringer et al., 2019; Steinmetz et al., 2019; Salkoff et al., 2020; Staudigl et al., 2022; for reviews, see Gothard, 2020; Wang, 2022).

In the perspective of neural oscillations, it has been known that brain-wide patterns of the oscillatory amplitude are related to behaviors. One well-known example can be found in the microstates of scalp electroencephalogram (EEG), which represent a finite number of spatial patterns of the EEG oscillatory amplitudes over the whole brain (Michel and Koenig, 2018). Individual EEG microstates reflect certain behavioral states during task performance, including mental arithmetic (Kim et al., 2021), audiovisual information integration (Wang et al., 2025), and the Stroop tasks (Barzon et al., 2024).

In particular, the naturalistic behavioral task maps from various behavioral information to different brain-wide patterns, because naturalistic behavior involves multiple cognitive processes that can induce multiple brain-wide patterns of neural activity (Samara et al., 2023). However, EEG microstates are difficult to apply for data recorded during naturalistic behavior, since naturalistic behaviors typically occur arbitrary timings whereas EEG microstate computation depends only on peak timings of EEG global power, leading to mismatches between these two timings. Therefore, it is necessary to devise a novel method based on oscillatory amplitudes that can afford any timings of occurrence of naturalistic behaviors.

* Corresponding author.
*E-mail address:* spkim@unist.ac.kr (S.-P. Kim).

https://doi.org/10.1016/j.neuroimage.2025.121521
Received 5 September 2025; Received in revised form 7 October 2025; Accepted 8 October 2025
Available online 9 October 2025

Meanwhile, brain-wide representations of behavior suggest that behavioral information should be effectively transmitted across distant brain areas. One proposed mechanism for this transmission is the propagation of brain oscillations–also known as traveling waves–which can mediate neural information transmission across brain areas (Rubino et al., 2006; Bhattacharya et al., 2022; Zabeh et al., 2023; for reviews, see Bauer et al., 2020; Kohn et al., 2020; Vinck et al., 2023). Recent traveling wave studies using human electrocorticography (ECoG) and EEG have explored how oscillatory propagation supports behavioral information transmission (for ECoG studies, see Zhang et al., 2018; Stolk et al., 2019; Halgren et al., 2019; Kleen et al., 2021; Mohan et al., 2024; for EEG studies, see Alamia and VanRullen, 2019; Pang et al., 2020; Alamia et al., 2020, 2023). For instance, in the human EEG studies, bottom-up visual information transmission through EEG oscillatory propagation is facilitated by visual stimulation (Pang et al., 2020) or psychedelic drug injection (Alamia et al., 2020).

Moreover, studies have revealed that local oscillatory propagation within a brain area is closely related to local oscillatory amplitudes. The strength of oscillatory propagation–often measured by spatial consistency of propagation directions over adjacent brain locations–is positively correlated with local oscillatory amplitudes in non-human primate local field potentials (LPFs) (Denker et al., 2018) and human ECoG (Das et al., 2022). However, for the human scalp EEG with standard electrode placement, such measurement of oscillatory propagation strength is limited due to low spatial resolution. Instead, temporal consistency of oscillatory propagation directions, which represents sustained oscillatory propagation in a particular period of interest, can characterize EEG oscillatory propagation, leveraging the high temporal resolution of EEG. Our prior study revealed that temporal consistency of local oscillatory propagation is positively correlated with local oscillatory amplitudes in human scalp EEG (Sihn and Kim, 2024). However, previous investigations have only focused on local brain regions, leaving open the question of how brain-wide patterns of oscillatory amplitude and oscillatory propagation interact with each other.

This study aims to investigate whether the brain-wide patterns of EEG oscillatory amplitudes can represent naturalistic behaviors. As EEG microstates are limited to be used for naturalistic behaviors, we propose a novel measurement of brain-wide patterns of oscillatory amplitudes based on the envelope of amplitudes. Specifically, we define putative oscillatory "activation states" according to the envelope of oscillatory amplitudes: active and inactive states. Then, we examine brain-wide patterns of these oscillatory activation states over the whole EEG channels. Also, we aim to examine the relationship between brain-wide patterns of the oscillatory active states and those of the temporal consistency of oscillatory propagation directions during naturalistic behaviors. Note that the envelope of oscillatory amplitudes used in the proposed activation states are preferred over the relative values of oscillatory amplitudes as used in microstates, when relating brain-wide patterns of oscillatory amplitudes to those of the temporal consistency of oscillatory propagation directions. For instance, the temporal consistency of oscillatory propagation directions can be simultaneously increased over whole brain regions. In this case, the relative values of oscillatory amplitudes cannot represent such patterns of temporal consistency as the gradient-like patterns of relative values cannot represent the uniform pattern of temporal consistency having no gradients. In contrast, the proposed activation states relaying on the absolute values of the envelope of oscillatory amplitudes can be mapped to any pattern of the temporal consistency of oscillatory propagation directions.

Various spatiotemporal characteristics of EEG has been widely used in the decoding of brain activity, including power spectrum, functional brain network, and neural manifold. For instance, periodic-aperiodic EEG measurements were developed to refine local EEG oscillatory amplitude and were used to validate the neural effects on acupuncture stimulation (Yu et al., 2024). While this method offers insights into refining our definition of "activation states" it is not optimized for measuring oscillatory amplitude that varies in the time domain, requiring further adjustment for its use. In addition to local EEG amplitudes, functional networks based on phase synchronization extracted from brain-wide EEG channels are altered by acupuncture stimulation or Alzheimer's disease (Yu et al., 2018; Yu et al., 2020). Because functional networks reflect EEG spatial patterns, temporal changes in functional networks can be seen as representing spatiotemporal features of neural information, similar to what we described using "activation states" in our study. However, the relationship between functional networks and brain-wide patterns of oscillatory amplitudes remains unclear. Recent studies use low-dimensional representations of EEG (i.e., neural manifolds) to decode external events (Yu et al., 2025). While, in principle, "activation states" can also be transformed into low-dimensional representations, due to the non-discrete nature of low-dimensional dynamics, it is necessary to further analyze relationships between the EEG oscillatory amplitude and the temporal consistency of EEG oscillatory propagations. Since temporal consistency could be defined on a definite domain, it can be directly calculated on discrete domains.

In this study, we used oscillatory amplitude to define "activation states" for neural representations of naturalistic behavior. Although oscillatory amplitude has been considered as a primary aspect of EEG oscillations, there are other types of information sources in EEG oscillations: frequency and phase (for a review, see Buzsáki et al., 2012). The reason why we adopt oscillatory amplitudes to define "activation states" was that not only they are traditionally considered as the primary aspect but also supported by many recent studies with the evidence that they can represent behaviors (Kim et al., 2021; Alasfour et al., 2022; Barzon et al., 2024; Yu et al., 2024; Bönstrup et al., 2025; Wang et al., 2025). However, the frequency information was also considered together in this study; "activation states" were separately defined in several frequency bands and were independently explored for the relationship with naturalistic behaviors. Furthermore, the phase information was used as a measure of oscillatory propagation, which was compared to "activation states".

For the investigation of naturalistic behaviors, we analyzed a publicly available dataset (Cavanagh and Castellanos, 2021) that consists of 63-channel scalp EEG recorded during video game play (Cavanagh and Castellanos, 2016). Behaviors observed in this video game play, such as pressing a missile launch button, collecting a star or an ammo box, crashing into wall or enemy, are more naturalistic than typical, well-controlled behaviors. These behaviors are not confined to a trial structure considered as statistically one sample, but rather are naturally occurring behaviors. Also, these behaviors are volitional without any external cues that are typically operationalized in controlled behaviors. Therefore, these behaviors are inherently naturalistic behaviors, rather than traditionally controlled ones. For some, playing video games may not be a daily activity, but rather a special behavior performed only in special circumstances. However, recent research has also determined behavior during video game play to be naturalistic (Alasfour et al., 2022). We tested whether the brain-wide patterns of oscillatory activation states could predict the likelihood of different naturalistic behaviors during video game play. Then, we compared these brain-wide patterns with those of the temporal consistency of oscillatory propagation.

## 2. Materials and methods

### 2.1. Dataset

In this study, we analyzed a publicly available dataset (Cavanagh and Castellanos, 2021), which can be accessed at: https://openneuro.org/datasets/ds003517/versions/1.1.0. This dataset consisted of 63-channel EEG recorded during video game play. The EEG data of 17 healthy participants (6 females) were included in this dataset. Participants were 29.94 × 5.02 years old on average. For 45 min, participants played the video game during which they drove a spacecraft, shoot missile to enemy spacecrafts, and avoided obstacles. When participants

played the video game, the events of 6 particular behaviors were recorded as follows: 1) "Missile launch button", 2) "Collect star", 3) "Collect ammo box", 4) "Crash into wall", 5) "Crash into enemy", and 6) "Missile hit enemy". The 63-channel EEG was recorded using the actiCHamp amplifier (actiCHamp, Brain Products GmbH, Germany) at a sampling rate of 500 Hz (Cavanagh and Castellanos, 2016).

### 2.2. EEG processing

Before applying the EEG artifact removal procedure, raw data underwent bandpass filtering at 0.5–50 Hz with a finite impulse response (FIR) filter (the order of 14 s). Then, eye-movement artifacts were removed by the Independent Component Analysis (ICA). The remaining artefacts were removed by the Artifact Subspace Reconstruction (ASR) procedure.

Afterward, we applied the surface Laplacian filtering to mitigate the volume conduction, using the CSD toolbox (Kayser and Tenke, 2006a, 2006b; Kayser, 2009). We set the parameters for CSD as $m = 4$ and $\lambda = 10^{-5}$, according to common setups in previous research on EEG oscillations (Tenke et al., 2011; Sihn et al., 2023; Sihn and Kim, 2024).

After the surface Laplacian filtering, we isolated delta, theta, alpha, and beta oscillations from the EEG data, using a FIR filter at 1–3 Hz, 4–7 Hz, 8–12 Hz, and 15–25 Hz, respectively. Filter orders were 7, 1.75, 0.875, and 0.4667 s, respectively. These bandpass-filtered data underwent Hilbert transform to extract both the oscillatory amplitude envelope and the oscillatory phase. After Hilbert transformation, EEG data was downsampled to 100 Hz. Note that we did not extract gamma oscillations since the envelope and phase of gamma oscillations in the scalp EEG recording are relatively unreliable due to vulnerability to noise.

### 2.3. Oscillatory activation state

We defined an oscillatory activation state based on the envelope of oscillatory amplitudes. For each frequency band, an oscillatory activation state at time $t$ was active if the amplitude envelope at time $t$ exceeded the median of amplitude envelopes for each participant during the whole period of video game play. Otherwise, it was defined as inactive. The state value was assigned to 1 for an active state, and −1 for an inactive state (Fig. 1A).

Next, we defined the brain-wide pattern of "active/inactive states". For each frequency band, we gathered multidimensional oscillatory activation states, where each dimension indicated each EEG channel, at every time point from all participants. Then, the k-means clustering algorithm was applied to these aggregated multidimensional oscillatory activation state data. The number of clusters ($K$) was varied from 2 to 10 according to previous studies on brain-wide patterns of oscillatory amplitude (Michel and Koenig, 2018; von Wegner et al., 2024; Tarailis et al., 2024). Then, for each participant, every time point was assigned to one of the clusters (Fig. 1B). Note that the clusters were formed across participants, comparable to the methods in previous studies (Gutierrez-Barragan et al., 2022; Michel and Koenig, 2018). A difference from previous studies was that the number of states in this study was fixed to 2: active and inactive states.

### 2.4. Oscillatory propagation analysis

To analyze EEG oscillatory propagation for each frequency band, we measured Local Phase Gradient (LPG) based on oscillatory phases (Fig. 2A and 2B), formed as a 3-dimensional vector (Sihn and Kim, 2024). Let $t$ be a time, $ch$ be an EEG channel of interest, and $chn$ be a neighboring channel of $ch$, where we used the nearest 8-channels. We represented left-right, anterior-posterior, and superior-inferior axes as $LR$, $AP$, and $SI$, respectively. Let $u_{XY}$ be an unit vector along with $XY$ axis, where $XY \in \{LR,\ AP,\ SI\}$. Let $\theta(ch,t)$ be an oscillatory phase at channel $ch$ at time $t$. Let $P(ch)$ be a 3-dimensional coordinate for the channel position. We calculated $\Delta\theta(chn,t) = \theta(chn,t) - \theta(ch,t)$, and $\Delta P_{XY}(chn) = P_{XY}(chn) - P_{XY}(ch)$ for each $chn$ where $P_{XY}$ indicates an 1-dimensional

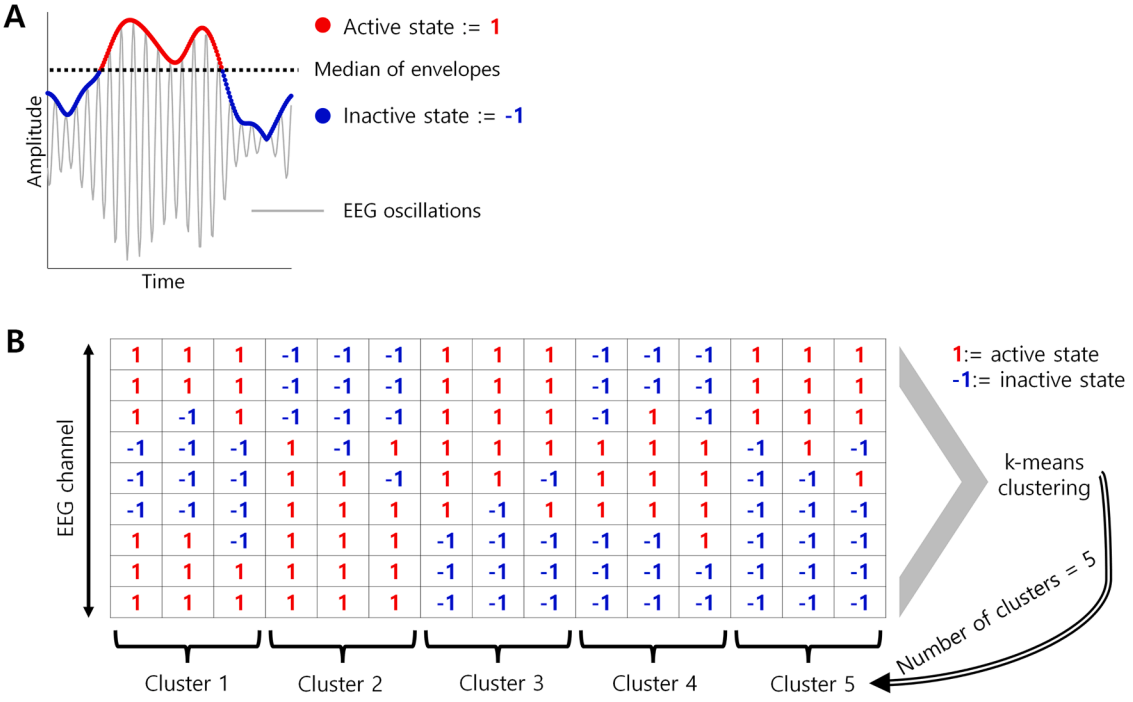


**Fig. 1. Illustrations of EEG oscillatory activation states.** (**A**) EEG oscillatory activation states were defined by the envelope of oscillatory amplitudes in a specific frequency band: active or inactive state if the envelope amplitude was higher or lower than median. Binary values of 1 and −1 were assigned to active and inactive states, respectively. (**B**) Brain-wide patterns of activation states from multidimensional oscillatory states (active state:= 1; inactive state:= −1), where each dimension indicates each EEG channel. The k-mean clustering algorithm was applied to group brain-wide patterns of activation states into $K$ clusters. In the example here, $K = 5$. For each participant and frequency band, a brain-wide pattern at every time point belongs to one of the clusters.

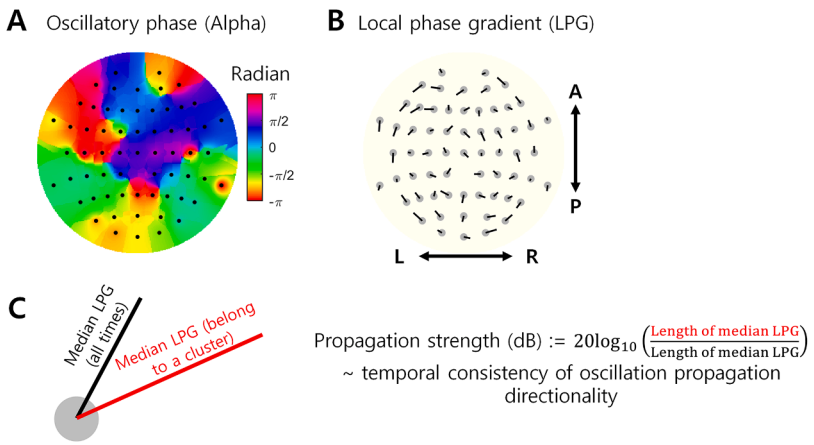


**Fig. 2.** Illustrations of EEG oscillatory propagation. (**A**) Example oscillatory phases. (**B**) Example local phase gradient (LPG) which quantifies the oscillatory propagation, and was calculated based on oscillatory phases. In A and B, each dot indicates each EEG channel. L, R, A, and P indicate left, right, anterior, and posterior, respectively. (**C**) Illustration of propagation strength: two different the median LPGs were obtained from time intervals when activation states belonged to a given cluster and from the whole time period that participants play the video game ("all times"). Propagation strength was defined as the ratio of participants-averaged median LPG lengths in decibels. It represented temporal consistency of oscillation propagation directionality.

coordinate for the channel position corresponding to $XY$ axis. Let $\rho_{XY}(ch,t)$ be a Pearson correlation between $\Delta\theta(chn,t)$ and $\Delta P_{XY}(chn)$ for each $chn$. Then, an LPG at channel $ch$ and time $t$ was given by (Fig. 2B):

$$LPG(ch,t) = \rho_{LR}(ch,t)u_{LR} + \rho_{AP}(ch,t)u_{AP} + \rho_{SI}(ch,t)u_{SI}. \quad (1)$$

The length of LPG was determined by $\rho_{XY}(ch,t)$, indicating that it represents the directional coherence of oscillatory propagation among neighboring channels rather than the propagation speed. If oscillatory propagation is consistent over a time interval, the directions of LPGs during that interval become consistent, making the aggregate of those LPGs would be larger. Therefore, we represented the temporal consistency of oscillatory propagation by the median value of LPGs. We calculated the median vector of LPG over time intervals with a certain condition:

$$mLPG(ch) = \text{median}\{LPG(ch,\ t) \mid t \text{ belongs to time intervals with a certain condition}\}. \quad (2)$$

The length of median LPG was obtained by:

$$LmLPG(ch) = \| mLPG(ch) \|_2 \quad (3)$$

Where $\| \cdot \|_2$ is an Euclidean norm. It reflected the temporal consistency of oscillatory propagation in a way that the larger the length was, the more temporally consistent oscillatory propagation was. The condition could vary depending on the purpose of oscillatory propagation analysis. Specifically, the condition could be oscillatory activation states (i.e., active vs. inactive) or the cluster of them.

As temporal consistency could indicate the strength of oscillatory propagation, we defined "propagation strength" at a channel $ch$ under a certain condition using $LmLPG(ch)$ as:

$$\Delta LmLPG(ch)_{\text{condition}} = 20\log_{10}\frac{\overline{LmLPG(ch)_{\text{conditton}}}}{\overline{LmLPG(ch)_{\text{whole}}}}, \quad (4)$$

where $\overline{(\cdot)}$ represents the average across participants. $LmLPG(ch)_{condition}$ is the length of median LPG obtained from all time intervals when a given condition was met, and $LmLPG(ch)_{whole}$ is that from the whole period of video game play. For instance, when the condition was the cluster of activation states, propagation strength when activation states belonged to a given cluster was calculated using equation (4) as shown in Fig. 2C.

### 2.5. Relation of brain-wide patterns of oscillatory activation states with behaviors

#### 2.5.1. Prediction of the likelihood of behaviors from brain-wide patterns of oscillatory activation states

As each cluster represents each brain-wide pattern of oscillatory activation states, we calculated the relative frequencies of individual clusters for each participant and frequency band. Let $c$ index a cluster and $N(c)$ be the number of appearances of the cluster $c$ during the video game play. Then, the relative frequency (RF) of the cluster $c$ was given by:

$$RF(c) = \frac{N(c)}{(1/K)\sum_{c'=1}^{K} N(c')} \quad (5)$$

where $K$ denotes the number of clusters. The $RF(c)$ was normalized such that the aggregate value across the clusters was equal to 1.

In the next step, we calculated the RF of behavior in association with the cluster for each participant and frequency band. Let $b$ index a behavior and $N(b,c)$ be the number of occurrences of the behavior $b$ when a cluster $c$ appeared during the video game play. The RF of the behavior $b$ in association with the cluster $c$ was given by:

$$RF(b;c) = \frac{N(b,\ c)}{(1/K)\sum_{c'=1}^{K} N(b,\ c')}. \quad (6)$$

Again, we normalized $RF(b;\ c)$ such that the aggregate value across the clusters was equal to 1.

Then, we examined dependency of the occurrence of the behavior $b$ on the cluster $c$. If the occurrence of $b$ was unrelated to $c$, the occurrence rate of $b$ in association with the cluster $c$ was expected exactly by the duration of $c$. Thus, $RF(b;\ c)$ would be equal to $RF(c)$. On the other hand, if the occurrence of $b$ was influenced by $c$, $RF(b;\ c)$ would be higher or

lower than $RF(c)$. Therefore, we measured a change in the RF of the behavior $b$ in association with the cluster $c$ as:

$$\Delta RF(b;c) = 20\log_{10}\frac{RF(b;c)}{RF(c)}. \quad (7)$$

This measure was represented as the decibel (dB) unit. The null hypothesis that the appearance of $c$ does not affect the occurrence of $b$ means $RF(b;\ c) = RF(c)$, making $\Delta RF(b;c) = 0$. The alternative hypothesis that the appearance of $c$ affects the occurrence of $b$ means $RF(b;c) \neq RF(c)$, making $\Delta RF(b;c) \neq 0$. As such, we statistically evaluated the change in the RF of the behavior $b$ in association with the cluster $c$ using the two-tailed Wilcoxon signed rank test. For multiple comparison, a p-value was false discovery rate (FDR)-corrected over behaviors and clusters.

#### 2.5.2. Decoding behavior from brain-wide patterns of oscillatory activation states

Here, we examined whether the brain-wide patterns of oscillatory activation states could encode behaviors. We conducted this examination via a decoding analysis, in which we attempted to discriminate oscillatory activation states according to behaviors. We aggregated all multidimensional oscillatory activation states from the periods of a certain behavior. We also averaged them over the periods of behavior–i.e., the mean activation state of the behavior. We performed two different decoding analyses.

First, we discriminated oscillatory activation states for a given frequency band occurring along with behavior, denoted as $S_{beh}$ here, from those occurring at random timings, denoted as $S_{rand}$. Let $MS_{beh}$ be a mean oscillatory activation state vector of $S_{beh}$ over the whole periods of the behavior. The dimensionality of these state vectors was equal to the number of EEG channels. We built a simple decoder to yield output as:

$$O_1(S_{beh},\ S_{rand}) = \begin{cases} Behavior,\ if\ S_{beh}\cdot MS_{beh} > S_{rand}\cdot MS_{beh} \\ Random,\ otherwise. \end{cases} \quad (8)$$

The decoding accuracy was set to the ratio of the number of times the output was "Behavior" over the total number of decoding trials.

Second, we classified oscillatory activation states in each frequency band into one of the 6 behaviors. Let $S_{beh(i)}$ be an oscillatory activation state vector occurring along with the $i$th behavior, and $MS_{beh(j)}$ be a mean oscillatory activation state vector of the $j$th behavior. A decoder produced output as:

$$O_2(S_{beh(i)}) = \arg\max_j S_{beh(i)}\cdot MS_{bev(j)}. \quad (9)$$

All decoding analyses were performed following 2-fold cross-validation.

### 2.6. Relations between the brain-wide patterns of oscillatory activation state and oscillatory propagation

To analyze whether the brain-wide patterns of the oscillatory activation states were related to those of oscillatory propagation, we examined the relationship between the multidimensional oscillatory activation states and the multidimensional temporal consistency of oscillatory propagation directionality. To this end, we aggregated all multidimensional oscillatory activation states on the time intervals belonging to a certain cluster, and averaged them over time and participants–i.e., the mean oscillatory activation state of that cluster. Next, we aggregated all LPGs at a given EEG channel ($ch$) during time intervals belonging to the same cluster, and calculated the median LPG, denoted as $mLPG(ch)_{cluster}$ (see equation (2)). We calculated the propagation strength under the condition of belonging to the cluster as (see equation (4) and Fig. 2C):

$$\Delta LmLPG(ch)_{cluster} = 20\log_{10}\frac{\|\overline{mLPG(ch)_{cluster}}\|_2}{\|\overline{mLPG(ch)_{whole}}\|_2}. \quad (10)$$

We represented a brain-wide pattern of oscillatory propagation by the vector of these propagation strength values from all channels. Then, we concatenated $K$ vectors of the mean oscillatory activation state across the clusters, where $K$ is the number clusters, and repeated it for the propagation strength. Then, we computed Pearson's correlation coefficient between this pair of concatenated vectors. We statistically evaluated the resulting correlation coefficient using a permutation test. To this end, a surrogate LPG was generated by either spatial or spatiotemporal permutations of EEG channels. The spatial permutation shuffled channels while preserving temporal patterns of LPG. In contrast, the spatiotemporal permutation shuffled both channels and temporal patterns of LPG. The number of surrogate LPGs was 1000.

## 3. Results

We first confirmed the existence of the relationship among the oscillatory amplitude, the oscillatory propagation, and behaviors in local brain regions using the data studied here. For these preliminary results, see supplementary materials.

### 3.1. Brain-wide patterns of oscillatory activation states represent behaviors

We investigated the appearance of each cluster of the brain-wide pattern of oscillatory activation states, in association with naturalistic behavior. We first observed that the mean oscillatory activation states for each cluster showed distinct brain-wide patterns (see Fig. 3A for an example of theta oscillations with the number of clusters set to 5). The analysis of the RF change of each behavior in association with clusters (see equation (6)) revealed that the occurrence of each behavior significantly depended on the appearance of clusters (Wilcoxon signed rank test, $p < 0.05$, FDR corrected, Fig. 3B). For the example in Fig. 3B, when the cluster 1 appeared, all the behaviors but the behavior 4 occurred less frequently. The occurrence of the behavior 4 was independent of the cluster 1. When the cluster 2 appeared, the behaviors 1, 2, 3 and 6 occurred more frequently whereas the behaviors 4 and 5 occurred less frequently. When the cluster 3 appeared, the behaviors 1 and 6 occurred more frequently whereas the other behaviors were independent of the cluster 3. When the cluster 4 appeared, all the behaviors occurred less frequently. When the cluster 5 appeared, all the behaviors occurred more frequently. When we randomly permuted the occurrence timing of clusters and reanalyzed the RF change of each behavior in association with clusters, behavior-cluster relationships observed in the original data above disappeared (Figure S4).

For each frequency band (delta, theta, alpha and beta) and cluster count ($K$), we measured the proportion of significant associations between behaviors and clusters. Specifically, we calculated the ratio of significant RF changes to the total number of combinations between behaviors and clusters. For the example in Fig. 3, there were 30 combinations of behaviors and clusters in total, among which the number of significant changes was 25, yielding the ratio of 83.33 %. The resulting ratios for all frequency bands and cluster counts were shown in Fig. 3C. Higher ratios of RF changes were observed in lower-frequency bands for all cluster counts. Remarkably, over 70 % of 60 combinations of behaviors and clusters showed significant associations even when the number of clusters increased to 10 in the brain-wide patterns of theta oscillations. In contrast, few significant associations were observed in those of higher-frequency bands such as beta oscillations. The results of RF changes demonstrated that the likelihood of the occurrence of naturalistic behaviors during video game play was dependent on the brain-wide patterns of oscillatory activation states, particularly in delta and theta bands.

Next, we conducted a series of decoding analyses to predict the occurrence of individual behaviors from the brain-wide patterns of oscillatory activation states. In the first decoding analysis, we discriminated the brain-wide patterns of oscillatory states during each behavior

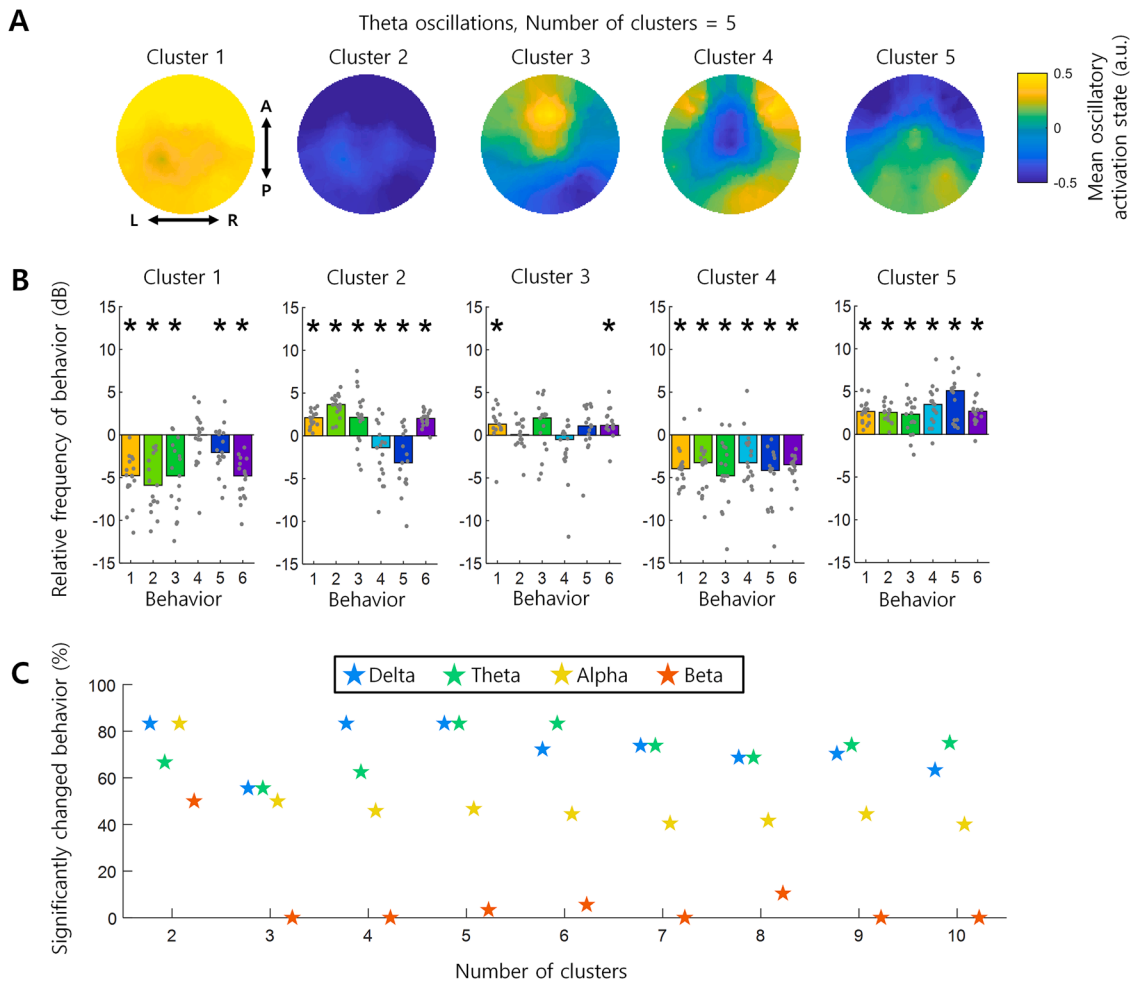


**Fig. 3. The likelihood of various behaviors was significantly dependent on the brain-wide coactivity pattern of oscillatory states.** (**A**) An example of brain-wide activity patterns. The distributions on EEG channels for the mean oscillatory activation state when the frequency band was set to theta oscillations and the number of clusters was 5. (**B**) The relative frequency of behavior in the case of A. Each dot indicates each participant and each bar indicates the median of the relative frequency of behavior. Asterisks indicate the statistical significance (two-tailed Wilcoxon signed rank test, $N = 17$, FDR-corrected $p < 0.05$). Behaviors 1 to 6 represent: {"Missile launch button", "Collect star", "Collect ammo box", "Crash into wall", "Crash into enemy", and "Missile hit enemy"}. (**C**) The ratio of significantly changed behavior. The significant change of behavioral occurrence indicates that the likelihood of the behavior was significantly dependent on the brain-wide pattern of oscillatory activation states.

from those at random timings using the mean oscillatory activation states of each behavior (see Fig. 4A). For every frequency band and behavior, decoding accuracies were significantly higher than the chance level (one-tailed Wilcoxon signed rank test, $N = 17$, $p < 0.05$) (Fig. 4B). We further inspected whether this discrimination of behavior-related patterns from random ones was specific to behaviors. In other words, we tested whether the decoding model discriminated brain-wide patterns related to any kind of behavior or those related to a particular behavior. Therefore, we performed an additional cross-behavior decoding analysis by building a decoding model (equation (8)) using the training data for one behavior (called 'model behavior') and applying it to the test data for another behavior (called 'sample behavior'). The result showed that decoding accuracy was relatively higher when the same behavior was used for both training and testing, as shown in Fig. 4B, than when different behaviors were used for training and testing respectively, in most cases of cross-behavior decoding (see Figure S5). It demonstrated that the discrimination of behavior-related activation states from randomly occurring ones was specific to behaviors.

In the second decoding analysis, we classified the brain-wide pattern of oscillatory states into one of the six behaviors, again using the mean oscillatory activation state of individual behaviors. The rates of correction classification were significantly higher than the chance level (approximately 0.166) for: the 2$^{nd}$ ("Collect star") and 5$^{th}$ (Crash into enemy) behaviors in delta oscillations, 4$^{th}$ ("Crash into wall") and 5th behaviors in theta oscillations, 3$^{rd}$ ("Collect ammo box"), 4$^{th}$ and 5$^{th}$ behaviors in alpha oscillations, and 3$^{rd}$, 4$^{th}$ and 5$^{th}$ behaviors in beta oscillations, respectively (one-tailed Wilcoxon rank sum test, $p < 0.05$) (Fig. 4C). The classification of the 1$^{st}$ ("Missile launch button") and 6$^{th}$ ("Missile hit enemy") behaviors did not exceed the chance level. These results revealed that the brain-wide pattern of oscillatory activation states could encode multiple naturalistic behaviors.

### 3.2. *Brain-wide patterns of oscillatory activation states and oscillatory propagation*

Next, we investigated the relationship between the brain-wide patterns of oscillatory activation states and those of the temporal consistency of oscillatory propagation directionality. We observed marked resemblance between the spatial pattern of oscillatory activation states and that of the propagation strength–i.e., cluster-conditioned temporal consistency of oscillatory propagation– in each cluster (see Fig. 5A, top and middle-upper for an example of alpha oscillations with the number of cluster set to 5). Such resemblance survived spatial permutation

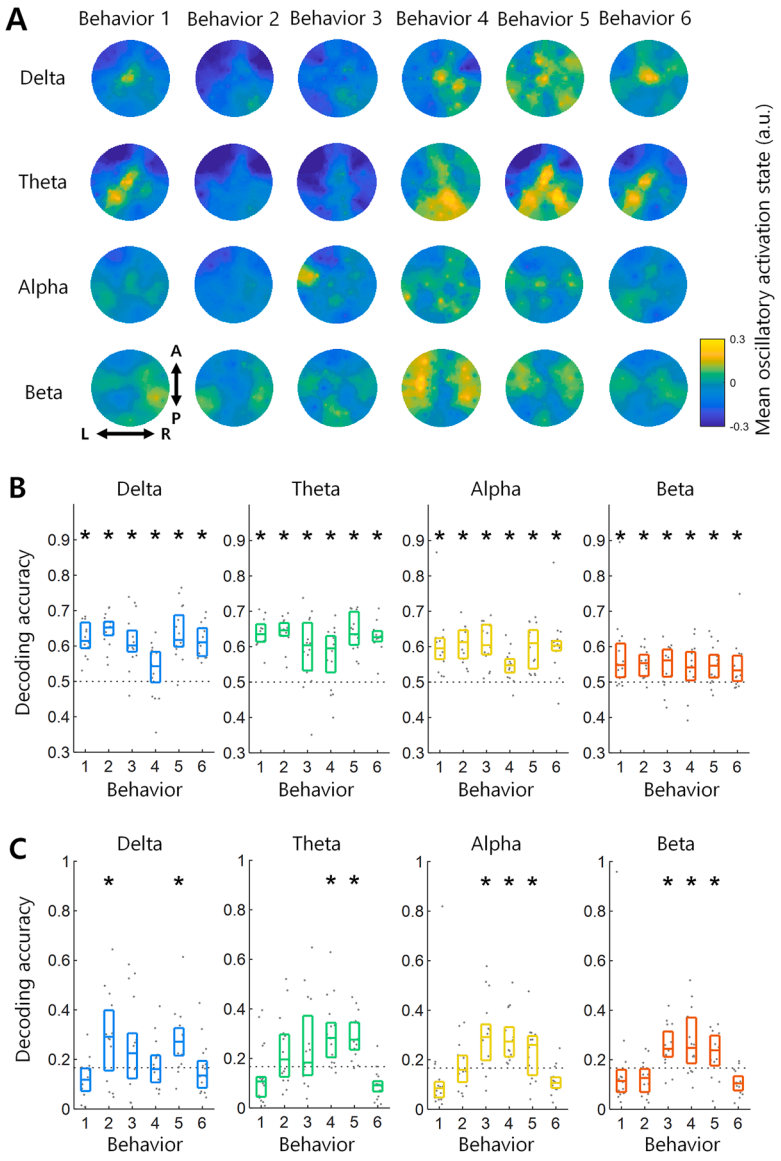


**Fig. 4. Decoding behavioral information from the brain-wide pattern of oscillatory states.** (**A**) Mean oscillatory activation states for each behavior in each frequency band. Behaviors 1 to 6 represent: {"Missile launch button", "Collect star", "Collect ammo box", "Crash into wall", "Crash into enemy", and "Missile hit enemy"}. (**B**) The accuracy of decoding the occurrence of individual behaviors relative to the occurrence of random events (see text). The accuracy of 1 means perfect decoding. Each dot indicates each participant and each dotted line indicates the chance level (50 %). Asterisks indicate significantly higher decoding accuracy than chance (one-tailed signed rank test, $N = 17$, $p < 0.05$). (**C**) The accuracy of decoding the brain-wide pattern of oscillatory states into one of the 6 behaviors. Asterisks indicate significantly higher decoding accuracy than chance (0.166) (one-tailed Wilcoxon rank sum test, $p < 0.05$).

(Fig. 5A middle-lower), but disappeared after spatiotemporal permutation (Fig. 5A bottom).

The correlation analysis across clusters revealed high correlations for every frequency band and cluster count (Pearson correlation, $N = 63 \times$ the number of clusters) (Fig. 5B). The mean CC over different cluster counts was 0.85 in delta, 0.88 in theta, 0.92 in alpha and 0.91 in beta, respectively. Positive correlations indicated that the propagation strength increased as mean oscillatory states became more active. The CCs from the original data were significantly higher than those from spatiotemporal permutated surrogate data for every frequency band and cluster count (Permutation test, $p < 0.05$). Furthermore, for most cases, the CCs from the original data were significantly higher than those from spatially permuted surrogate data (Permutation test, $p < 0.05$) (Fig. 5B).

## 4. Discussion

In this study, we investigated how the brain-wide patterns of EEG oscillations related to the likelihood of naturalistic behaviors occurring during video game play. To characterize the brain-wide patterns in specific frequency bands, we defined the activation states of oscillations based on the envelope of oscillatory amplitudes, with states classified as active when the envelope exceeded the median and inactive otherwise (Fig. 1). Then, we clustered whole-channel activation states to derive brain-wide patterns, analogous to finding EEG microstates. The results revealed that the likelihood of the occurrence of particular behaviors was associated with the brain-wide patterns of oscillatory activation states (Fig. 3). Stronger associations were observed in lower-frequency oscillations (delta and theta) compared to higher-frequency ones (alpha and beta). Further decoding analyses supported this association, revealing that behavioral occurrences could be inferred from the brain-wide oscillatory activation patterns (Fig. 4).

Our finding is consistent with previous studies using microstates or the hidden Markov model (HMM). For example, studies have shown that the brain-wide patterns of oscillatory states, which were either

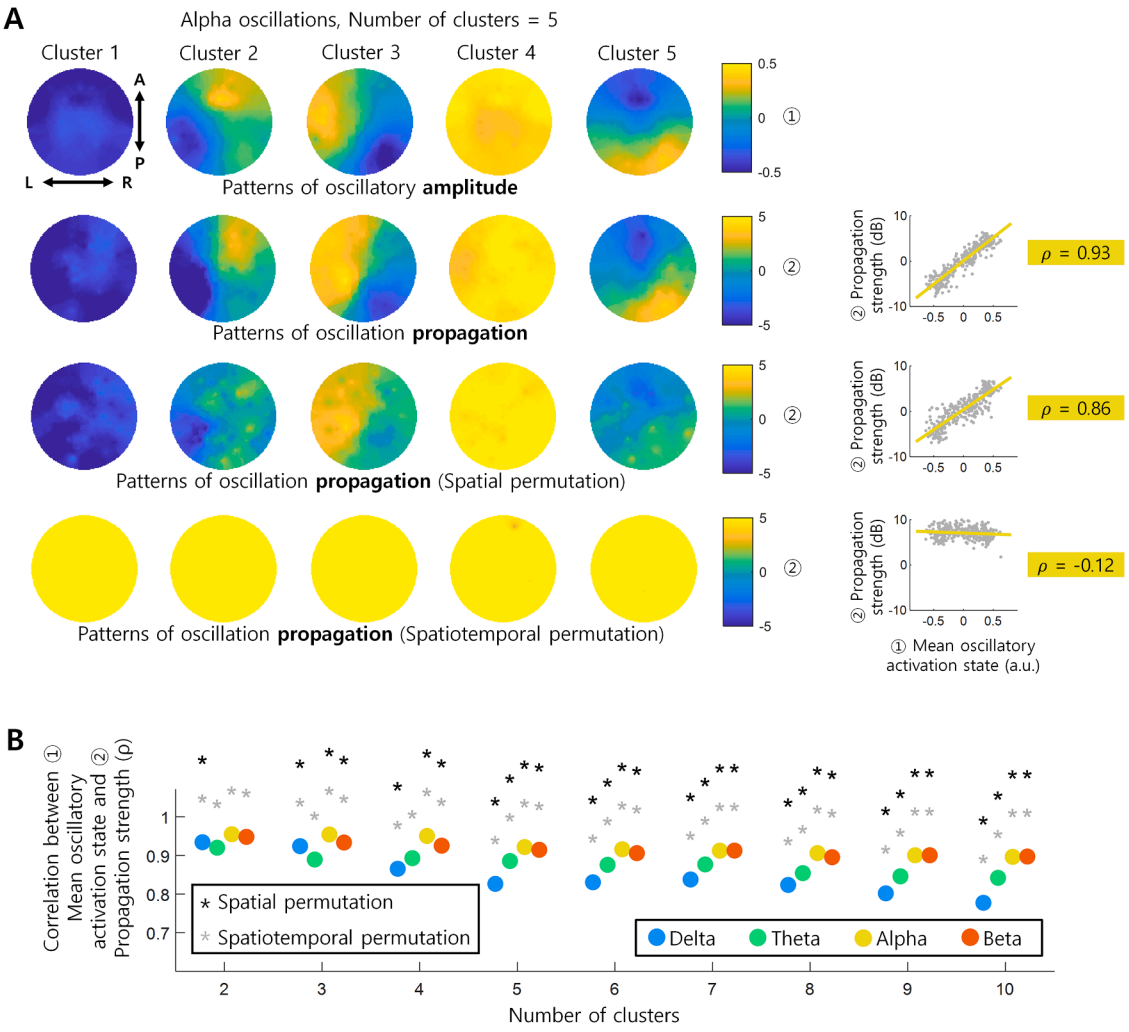


**Fig. 5. Correlations between the brain-wide patterns of oscillatory activation states and oscillatory propagation.** (**A**) An example of brain-wide patterns for alpha oscillations with 5 clusters. (top) The brain-wide spatial pattern of the mean oscillatory activation state for each cluster. A, P, L and R denote anterior, posterior, left and right, respectively. (middle-upper) The brain-wide spatial pattern of the propagation strength for each cluster, which represented temporal consistency of oscillatory propagation directionality when the activation state belonged to that cluster. The unit of propagation strength is dB. In the right panel, each dot indicates each EEG channel from one of the clusters ($N = 315$ (63 channels with 5 clusters)). $\rho$ represents Pearson's correlation coefficient between the cluster-aggregated spatial pattern of the mean oscillatory activation state and that of the propagation strength. (middle-lower) The brain-wide spatial pattern of the propagation strength for each cluster, where the local phase gradients (LPGs) were obtained from spatially permutated surrogate data. (bottom) The brain-wide spatial pattern of the propagation strength for each cluster from spatiotemporally permutated surrogate data. (**B**) Pearson's correlation coefficients between the cluster-aggregated spatial pattern of the mean oscillatory activation state and that of the propagation strength for each frequency band across different numbers of clusters. The asterisk indicates the significance of correlation coefficients compared to surrogate LPGs generated by spatial or spatiotemporal permutations (Permutation test, $p < 0.05$).

microstates or latent states inferred from HMM, were associated with behavioral performance of reasoning or motor imagery (Zappasodi et al., 2019; Liu et al., 2024). Other studies revealed that the brain-wide patterns of oscillatory microstates or transient states were associated with various neurological and psychiatric disorders such as schizophrenia, major depressive disorder, Alzheimer's disease, Parkinson's disease, and consciousness disorders (Soni et al., 2019; Li et al., 2023; Lian et al., 2021; Lamoš et al., 2023; Bai et al. 2021). In line with the previous studies, this study demonstrated that the brain-wide patterns of oscillatory activation states represented *naturalistic* behaviors. Since microstates could not be employed for such behaviors that occurred naturally with no controlled timings, we developed oscillatory activation states to find brain-wide patterns.

In the aforementioned studies of EEG microstates and HMM (Zappasodi et al., 2019; Liu et al., 2024), including our study, the relationship between behaviors and brain-wide "coactivity" patterns was inferred through clustering algorithms. Among these studies on "coactivity" patterns, our study uniquely deals with naturalistic behaviors (Fig. 3). If it is possible to dissect naturalistic behaviors as a combination of specific behavioral information, we can interpret our results as the consequence of a combination of previous findings on brain-wide "coactivity" patterns. However, such dissection remains elusive for naturalistic behaviors studied here, hindering direct alignment of our result on previous ones. On the other hands, the relationship between naturalistic behaviors and brain-wide "channel-wise average" patterns has been investigated. For instance, a recent study on naturalistic motor behaviors, such as "phone lifting", "spiral drawing", and "typing", reported the representation of these behaviors in the brain-wide amplitude patterns of theta, alpha, and beta oscillations in EEG (Bönstrup et al., 2025). These results are comparable to our results that brain-wide "channel-wise average" patterns represented different gameplay behaviors, which varied across EEG oscillations (Fig. 4A). Since both studies include naturalistic "motor" behaviors, our results are partly in line with the results of previous study. Moreover, a recent intracranial

EEG (iEEG) study showed that brain-wide patterns of the amplitudes of high gamma activity can be decoded into naturalistic behaviors such as "engaging in dialogue" and "using electronics" (Alasfour et al., 2022). This result is comparable to our result that different behaviors could be decodable from brain-wide "channel-wise average" patterns (Fig. 4C), together indicating distinctive brain-wide "channel-wise average" patterns during different behaviors.

Several brain-wide EEG features have been used in decoding neural information, for examples, power spectrum (Yu et al., 2024), functional brain network (Yu et al., 2020), and neural manifold (Yu et al., 2025). This ability of decoding EEG features can provide a basis for EEG-based brain-computer interface (BCI) systems. When one designs BCIs to translate EEG patterns into naturalistic behaviors, the features of brain-wide patterns may have a more flexibility than traditional features for decoding naturalistic behaviors; since the number of naturalistic behaviors may be varied. In this circumstance, our method could be applied to decoding naturalistic behaviors through adjusting the optimal number of clusters in accordance with the number of behaviors. However, EEG microstates can also be used equally for this purpose, as they have been used in decoding neural information such as speech perception and neuropsychological biomarkers (Duc and Lee, 2020; for a review, see Asha et al., 2024). Nonetheless, the advantage of our method over EEG microstates lies in the connection between brain-wide activation patterns and oscillatory propagations (Fig. 5), which will enrich the number of features available for decoding. As such, to build BCI systems for naturalistic behavior, we may propose a model that uses both brain-wide activation and oscillatory propagation patterns. This model might be advantageous in decoding more complex naturalistic behaviors using a larger number of brain-wide "coactivity" patterns and have abundant propagation patterns.

Recent findings that neural representations of various behaviors are distributed throughout the whole brain (Kaplan and Zimmer, 2020; Westlin et al., 2023) indicate that neural information of behaviors needs to be transmitted throughout the brain. Since the propagation of brain oscillations mediates neural information transmission (Rubino et al., 2006; Bhattacharya et al., 2022; Zabeh et al., 2023; Vinck et al., 2023), we examined the relationship between the brain-wide patterns of oscillatory propagation with those of oscillatory activation states. To this end, we characterized EEG oscillatory propagation at each channel using local phase gradients and defined propagation strength that represented temporal consistency of propagation directionality (Fig. 2). We found high correlations (0.85 ~ 0.92) between the brain-wide patterns of propagation strength and those of oscillatory activation states in every frequency band (Fig. 5). Furthermore, we also found that the directionality of local oscillatory propagation was related to behavioral information processing (Figure S3).

The temporal consistency of oscillatory propagation directionality increased when the oscillatory state was active. This means that increased oscillatory amplitudes might support persistent oscillatory propagation in a particular direction. It is noteworthy that although we defined active/inactive states simply based on the median of amplitude envelopes, which seemed somewhat arbitrary, these states could correspond to neural information processing represented by the oscillatory propagation. Previous studies also reported that high-amplitude states promote the spatial consistency of oscillatory propagation in monkey local field potential (LPF) (Denker et al., 2018) and human ECoG (Das et al., 2022). Taken together, high-amplitude "active states" –i.e., synchronized neuronal units– may support spatio-temporally consistent oscillatory propagation. As the brain-wide patterns of activation states were closely related to the likelihood of behaviors (Figs. 3 and S3), the generation of brain oscillations from synchronized neuronal units may be related to the propagation of neural information of behaviors.

The high correlations between the brain-wide patterns of propagation strength and those of oscillatory activation states observed in the original data did not reduce much when the data were spatially permuted, but drastically reduced when spatiotemporally permuted (Figure S6). This indicates that when surrogate LPGs were generated by shuffling channel locations through spatial permutation, destroying neighborhood of original EEG channels while preserving temporal structures, temporal consistency of propagation directionality did not decrease substantially. It implies that propagation strength defined in this study might be more dependent on temporal structure of LPGs than spatial phase relations. Nonetheless, correlation coefficients from the original data were still significantly higher than those from spatially permuted data (Fig. 5B). It verifies the existence of significant coupling between oscillatory amplitudes and propagation directionality at a brain-wide level.

Gap junctions between inhibitory interneurons are thought to play a key role in the generation of these brain oscillations (Szabadics et al., 2001; Roopun et al., 2006; Phookan et al., 2015). Since these gap junctions connect interneurons of the same type within a cortical layer (Hestrin and Galarreta, 2005; Coulon and Landisman, 2017), brain oscillations may arise independently across layers. Such layer-specific brain oscillations could propagate though the brain to independently transmit distinct streams of behavioral information. This view is supported by evidence that brain oscillations in different frequency bands preferentially dominate separate cortical layers (Gieselmann et al., 2022), suggesting frequency-specific contribution of brain oscillations to behavior. Therefore, neural information of individual behaviors would be transmitted independently throughout the brain via the propagation of layer-, and frequency-specific brain oscillations.

In this study, we observed that low-amplitude, inactive oscillatory states reduced the temporal consistency of oscillatory propagation (Figs. 5 and S3). Such reductions in amplitude, reflecting desynchronization of neuronal activities, may indicate a distinct brain function beyond the mere propagation of behavioral information. One possibility is that disinhibition of interneurons can weaken oscillatory amplitudes, facilitating information transfer between distinct neuronal populations

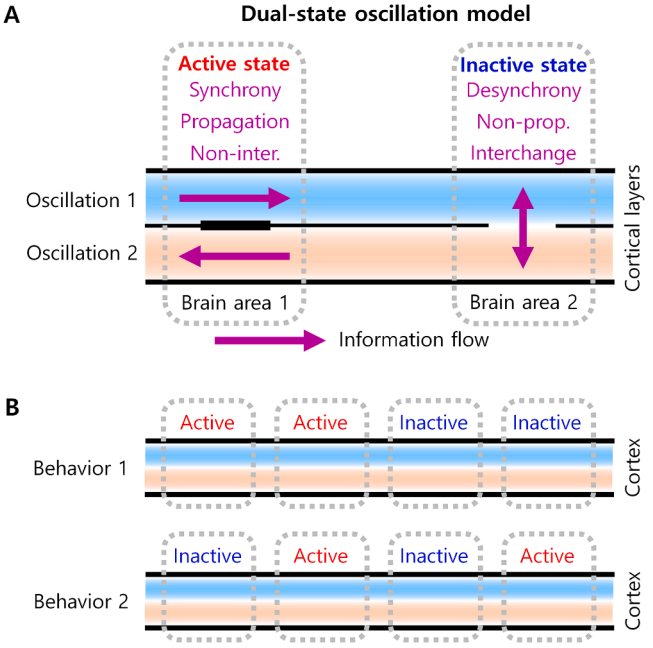


**Fig. 6. Dual-state oscillation model for behavioral information processing.** (**A**) During high amplitude "active state", i.e., a period that a large portion of neurons are synchronized, behavioral information is propagated throughout the brain. During low amplitude "inactive state", i.e., a period that a large portion of neurons are desynchronized, various bodies of behavioral information are interchanged among them. (**B**) Different behaviors have different brain-wide patterns of oscillatory states, which are combinations of "active state" and "inactive state" in many brain areas.

(Wang and Yang, 2018; Guet-McCreight et al., 2020). This mechanism could relate to mixed selectivity, in which a single neuron encodes multiple types of information (Rigotti et al., 2013; Aoi et al., 2020; Fusi et al., 2016; Gothard, 2020). From this perspective, inactive oscillatory states may support transient information exchange across different neural domains presumably related to different behaviors. Building on these, we propose a "dual-state oscillation model (DSOM)," in which active-state oscillations support the propagation of specific behavioral information across brain areas, whereas inactive-state oscillations enable information interchange between different neural populations within a local area (Fig. 6A). The brain-wide patterns of oscillatory activation states observed in this study may therefore reflect distributed neural information processing including both global information propagation and local information exchange for integrating behavioral information (Fig. 6B).

In sum, we defined "activation states" based on oscillatory amplitudes and obtained brain-wide patterns of them. In fact, these brain-wide patterns represented the global patterns of local oscillatory amplitude levels. The high and low local amplitude levels corresponded to active and inactive states, respectively. The active state corresponds to the state that pyramidal neurons are synchronized by concurrently activated inhibitory interneurons with gap junctions (Szabadics et al., 2001; Roopun et al., 2006; Phookan et al., 2015). Since neurons are synchronized, neural information transferred by those neurons could easily be propagated to other regions, as demonstrated by the present study (Fig. 5), as well as the previous studies (Denker et al., 2018; Das et al., 2022). In contrast, the inactive state corresponds to the state that inhibitory interneurons are inhibited so that pyramidal neurons are disinhibited and thus desynchronized. As a result, the information propagation between regions is limited, which is observed by the limited oscillatory propagations in the present study (Fig. 5) as well as the previous ones (Denker et al., 2018; Das et al., 2022). Instead, information interchange between other populations of pyramidal neurons is facilitated by disinhibition (Wang and Yang, 2018; Guet-McCreight et al., 2020), which would result in mixed-selectivity in which a single neuron encodes multiple types of information (Rigotti et al., 2013; Aoi et al., 2020; Fusi et al., 2016; Gothard, 2020).

For the active and inactive states, the key players are inhibitory interneurons with gap junctions that connect interneurons of the same type within a cortical layer (Hestrin and Galarreta, 2005; Coulon and Landisman, 2017), inducing functionally separated populations in each cortical layer. The combination of activation states of these populations across the brain regions and cortical layers can be expressed as a behavioral state, since the brain function can be considered partially localized (Béna and Goodman, 2025) and the combination of these differently localized behavioral functions could represent various behaviors. This combination corresponds to each brain-wide pattern of activation states, which was shown to be related to naturalistic behaviors in this study (Figs. 3 and 4). It is noteworthy that both brain-wide patterns of activation states and EEG microstates are based on EEG oscillatory amplitude. However, since EEG microstates are defined solely on the peaks of global field power (Michel and Koenig, 2018), it lacks the explanation of a state low amplitudes in every brain region. In contrast, the brain-wide patterns of activation states can accommodate all types of combinations so as to represent putatively a variety of behaviors.

### 4.1. Limitations

As this study basically investigated relationships among brain-wide patterns of oscillatory states, oscillatory propagation and behavioral performances, no comprehensive model for brain-wide patterns and behavioral information processing is provided. Future studies may elaborate on the comprehensive understanding of how brain-wide patterns of oscillatory states lead to certain behavioral performance.

In addition, this study used fixed frequencies for all individuals and brain regions to effectively control the frequency range of EEG oscillations. However, it is generally known that the central frequency of EEG oscillations varies across individuals and brain regions (Haegens et al., 2014). Therefore, future studies could replicate the results of this study by using differentiated frequencies for each individual and brain region.

Finally, the volume conduction problem of scalp EEG could lead to a wrong interpretation of spatial patterns of active/inactive states. Although we minimized the volume conduction effect through surface Laplacian filtering, it may not be sufficient to rule out the effect completely. Future studies using neuroimaging methods of high spatial resolution such magnetoencephalography (MEG) may address the volume conduction issue more appropriately.

### 4.2. Conclusions

In this study, we demonstrated that the brain-wide patterns of EEG oscillatory activation states, derived from oscillatory amplitude envelope, could represent naturalistic behaviors occurring during video game play. We also showed high correlations between the brain-wide patterns of oscillatory activation states and those of oscillatory propagation directionality such that oscillatory propagation became more persistent when oscillatory state was more active. Based on these key findings, we proposed a dual-state oscillation model (DSOM) to depict neural processing of naturalistic behavior. In DSOM, behavioral information would be propagated inter-regionally during active states while being interchanged between neuronal populations intra-regionally during inactive state. As naturalistic behavior involves various cognitive and affective processes recruiting diverse neural assemblies over the whole brain, the brain-wide patterns of oscillatory activation states may help to illuminate neural correlates of naturalistic behavior effectively. Moreover, we anticipate that examination of the brain-wide patterns of oscillatory activation states together with DSOM may offer a unique means to diagnose the brain functions in people with neurological disorders in naturalistic daily environments.

## Ethics statement

The experiment to obtain the original dataset was approved by the University of New Mexico (UNM) Institutional Review Board and every participant submitted written informed consent (Cavanagh and Castellanos, 2016). Since this study used only a publicly available dataset, ethical approval for this study involving humans is exempt by the local legislation (Article 13, Paragraph 1, Subparagraph 3 of the Enforcement Rule of Bioethics and Safety Act of the Republic of Korea).

## Data and code availability statement

The data used in this study are publicly available and can be downloaded at: https://openneuro.org/datasets/ds003517/versions/1.1.0. The analysis code used in this study is available from the corresponding author upon request.

## CRediT authorship contribution statement

**Duho Sihn:** Writing – review & editing, Writing – original draft, Visualization, Validation, Supervision, Software, Resources, Project administration, Methodology, Investigation, Funding acquisition, Formal analysis, Data curation, Conceptualization. **Sung-Phil Kim:** Writing – review & editing, Writing – original draft, Visualization, Supervision, Project administration, Funding acquisition.

## Declaration of competing interest

The authors declare that they have no known competing financial interests or personal relationships that could have appeared to influence the work reported in this paper.

## Acknowledgements

This research was supported by the National Research Foundation of Korea (NRF) grant funded by the Korea government (MSIT) (No. RS-2023–00213187 and RS-2025–00522357).

## Supplementary materials

Supplementary material associated with this article can be found, in the online version, at doi:10.1016/j.neuroimage.2025.121521.

## References

Alamia, A., Terral, L., D'ambra, M.R., VanRullen, R., 2023. Distinct roles of forward and backward alpha-band waves in spatial visual attention. eLife 12, e85035. https://doi.org/10.7554/eLife.85035.

Alamia, A., Timmermann, C., Nutt, D.J., VanRullen, R., Carhart-Harris, R.L., 2020. DMT alters cortical travelling waves. eLife 9, e59784. https://doi.org/10.7554/eLife.59784.

Alamia, A., VanRullen, R., 2019. Alpha oscillations and traveling waves: signatures of predictive coding? PLoS Biol. 17, e3000487. https://doi.org/10.1371/journal.pbio.3000487.

Alasfour, A., Gabriel, P., Jiang, X., Shamie, I., Melloni, L., Thesen, T., Dugan, P., Friedman, D., Doyle, W., Devinsky, O., Gonda, D., Sattar, S., Wang, S., Halgren, E., Gilja, V., 2022. Spatiotemporal dynamics of human high gamma discriminate naturalistic behavioral states. PLoS Comput. Biol. 18, e1010401. https://doi.org/10.1371/journal.pcbi.1010401.

Aoi, M.C., Mante, V., Pillow, J.W., 2020. Prefrontal cortex exhibits multidimensional dynamic encoding during decision-making. Nat. Neurosci. 23, 1410–1420. https://doi.org/10.1038/s41593-020-0696-5.

Asha, S.A., Sudalaimani, C., Devanand, P., Alexander, G., Arya, M.L., Sanjeev, V.T., Ramshekhar, N.M., 2024. Analysis of EEG microstates as biomarkers in neuropsychological processes – Review. Comput. Biol. Med. 173, 108266. https://doi.org/10.1016/j.compbiomed.2024.108266.

Bai, Y., He, J., Xia, X., Wang, Y., Yang, Y., Di, H., Li, X., Ziemann, U., 2021. Spontaneous transient brain states in EEG source space in disorders of consciousness. NeuroImage 240, 118407. https://doi.org/10.1016/j.neuroimage.2021.118407.

Barzon, G., Ambrosini, E., Vallesi, A., Suweis, S., 2024. EEG microstate transition cost correlates with task demands. PLoS Comput. Biol. 20, e1012521. https://doi.org/10.1371/journal.pcbi.1012521.

Bauer, A.-K.R., Debener, S., Nobre, A.C., 2020. Synchronisation of neural oscillations and cross-modal influences. Trends Cogn. Sci. (Regul. Ed.) 24, 481–495. https://doi.org/10.1016/j.tics.2020.03.003.

Béna, G., Goodman, D.F.M., 2025. Dynamics of specialization in neural modules under resource constraints. Nat. Commun. 1, 187. https://doi.org/10.1038/s41467-024-55188-9.

Bhattacharya, S., Brincat, S.L., Lundqvist, M., Miller, E.K., 2022. Traveling waves in the prefrontal cortex during working memory. PLoS Comput. Biol. 18, e1009827. https://doi.org/10.1371/journal.pcbi.1009827.

Bönstrup, M., Schneider, T., Bräuer, A., Ader, J., Villringer, A., Classen, J., 2025. Brain-wide spatial mapping of oscillatory activity during naturalistic motor behavior. J. Neurophysiol. 133, 1583–1593. https://doi.org/10.1152/jn.00500.2024.

Buzsáki, G., Anastassiou, C.A., Koch, C., 2012. The origin of extracellular fields and currents — EEG, ECoG, LFP and spikes. Nat. Rev. Neurosci. 13, 407–420. https://doi.org/10.1038/nrn3241.

Cavanagh, J.F., Castellanos, J., 2016. Identification of canonical neural events during continuous gameplay of an 8-bit style video game. NeuroImage 133, 1–13. https://doi.org/10.1016/j.neuroimage.2016.02.075.

Cavanagh, J.F., Castellanos, J., 2021. EEG: continuous gameplay of an 8-bit style video game. OpenNeuro. https://doi.org/10.18112/openneuro.ds003517.v1.1.0 (Available from: https://openneuro.org/datasets/ds003517/versions/1.1.0. </Dataset>.

Coulon, P., Landisman, C.E., 2017. The potential role of gap junctional plasticity in the regulation of state. Neuron 93, 1275–1295. https://doi.org/10.1016/j.neuron.2017.02.041.

Das, A., Myers, J., Mathura, R., Shofty, B., Metzger, B.A., Bijanki, K., Wu, C., Jacobs, J., Sheth, S.A., 2022. Spontaneous neuronal oscillations in the human insula are hierarchically organized traveling waves. eLife 11, e76702. https://doi.org/10.7554/eLife.76702.

Denker, M., Zehl, L., Kilavik, B.E., Diesmann, M., Brochier, T., Riehle, A., Grün, S., 2018. LFP beta amplitude is linked to mesoscopic spatio-temporal phase patterns. Sci. Rep. 8, 5200. https://doi.org/10.1038/s41598-018-22990-7.

Duc, N.T., Lee, B., 2020. Decoding brain dynamics in speech perception based on EEG microstates decomposed by multivariate Gaussian hidden Markov model. IEEE Access 8, 146770–146784. https://doi.org/10.1109/ACCESS.2020.3015292.

Fusi, S., Miller, E.K., Rigotti, M., 2016. Why neurons mix: high dimensionality for higher cognition. Curr. Opin. Neurobiol. 37, 66–74. https://doi.org/10.1016/j.conb.2016.01.010.

Gieselmann, M.A., Thiele, A., 2022. Stimulus dependence of directed information exchange between cortical layers in macaque V1. eLife 11, e62949. https://doi.org/10.7554/eLife.62949.

Gothard, K.M., 2020. Multidimensional processing in the amygdala. Nat. Rev. Neurosci. 21, 565–575. https://doi.org/10.1038/s41583-020-0350-y.

Guet-McCreight, A., Skinner, F.K., Topolnik, L., 2020. Common principles in functional organization of VIP/Calretinin cell-driven disinhibitory circuits across cortical areas. Front Neural Circuits 14, 32. https://doi.org/10.3389/fncir.2020.00032.

Gutierrez-Barragan, D., Singh, N.A., Alvino, F.G., Coletta, L., Rocchi, F., De Guzman, E., Galbusera, A., Uboldi, M., Panzeri, S., Gozzi, A., 2022. Unique spatiotemporal fMRI dynamics in the awake mouse brain. Curr. Biol. 32, 631–644. https://doi.org/10.1016/j.cub.2021.12.015.

Haegens, S., Cousijn, H., Wallis, G., Harrison, P.J., Nobre, A.C., 2014. Inter- and intra-individual variability in alpha peak frequency. NeuroImage 92, 46–55. https://doi.org/10.1016/j.neuroimage.2014.01.049.

Halgren, M., Ulbert, I., Bastuji, H., Fabó, D., Erőss, L., Rey, M., Devinsky, O., Doyle, W.K., Mak-McCully, R., Halgren, E., Wittner, L., Chauvel, P., Heit, G., Eskandar, E., Mandell, A., Cash, S.S., 2019. The generation and propagation of the human alpha rhythm. Proc. Natl. Acad. Sci. 116, 23772–23782. https://doi.org/10.1073/pnas.1913092116.

Hestrin, S., Galarreta, M., 2005. Electrical synapses define networks of neocortical GABAergic neurons. Trends Neurosci. 28, 304–309. https://doi.org/10.1016/j.tins.2005.04.001.

Kaplan, H.S., Zimmer, M., 2020. Brain-wide representations of ongoing behavior: a universal principle? Curr. Opin. Neurobiol. 64, 60–69. https://doi.org/10.1016/j.conb.2020.02.008.

Kayser, J., Tenke, C.E., 2006a. Principal components analysis of Laplacian waveforms as a generic method for identifying ERP generator patterns: I. Evaluation with auditory oddball tasks. Clin. Neurophysiol. 117, 348–368. https://doi.org/10.1016/j.clinph.2005.08.034.

Kayser, J., Tenke, C.E., 2006b. Principal components analysis of Laplacian waveforms as a generic method for identifying ERP generator patterns: II. Adequacy of low-density estimates. Clin. Neurophysiol. 117, 369–380. https://doi.org/10.1016/j.clinph.2005.08.03332.

Kayser, J., 2009. Current Source Density (CSD) Interpolation Using Spherical Splines - CSD toolbox (Version 1.1). New York State Psychiatric Institute: Division of Cognitive Neuroscience. [Software]. Available at: http://psychophysiology.cpmc.columbia.edu/Software/CSDtoolbox.

Kim, K., Duc, N.T., Choi, M., Lee, B., 2021. EEG microstate features according to performance on a mental arithmetic task. Sci. Rep. 11, 343. https://doi.org/10.1038/s41598-020-79423-7.

Kleen, J.K., Chung, J.E., Sellers, K.K., Zhou, J., Triplett, M., Lee, K., Tooker, A., Haque, R., Chang, E.F., 2021. Bidirectional propagation of low frequency oscillations over the human hippocampal surface. Nat. Commun. 12, 2764. https://doi.org/10.1038/s41467-021-22850-5.

Kohn, A., Jasper, A.I., Semedo, J.D., Gokcen, E., Machens, C.K., Yu, B.M., 2020. Principles of corticocortical communication: proposed schemes and design considerations. Trends Neurosci. 43, 725–737. https://doi.org/10.1016/j.tins.2020.07.001.

Lamoš, M., Bočková, M., Goldemundová, S., Baláž, M., Chrastina, J., Rektor, I., 2023. The effect of deep brain stimulation in Parkinson's disease reflected in EEG microstates. npj Parkinson's Disease. 9, 63. doi: 10.1038/s41531-023-00508-x.

Li, J., Li, N., Shao, X., Chen, J., Hao, Y., Li, X., Hu, B., 2023. Altered brain dynamics and their ability for major depression detection using EEG microstates analysis. IEEE Trans. Affect Comput. 14, 2116–2126. https://doi.org/10.1109/TAFFC.2021.3139104.

Lian, H., Li, Y., Li, Y., 2021. Altered EEG microstate dynamics in mild cognitive impairment and Alzheimer's disease. Clin. Neurophysiol. 132, 2861–2869. https://doi.org/10.1016/j.clinph.2021.08.015.

Liu, Y., Yu, S., Li, J., Ma, J., Wang, F., Sun, S., Yao, D., Xu, P., Zhang, T., 2024. Brain state and dynamic transition patterns of motor imagery revealed by the bayes hidden markov model. Cogn Neurodyn. 18, 2455–2470. https://doi.org/10.1007/s11571-024-10099-9.

Michel, C.M., Koenig, T., 2018. EEG microstates as a tool for studying the temporal dynamics of whole-brain neuronal networks: a review. NeuroImage 180, 577–593. https://doi.org/10.1016/j.neuroimage.2017.11.062.

Mohan, U.R., Zhang, H., Ermentrout, B., Jacobs, J., 2024. The direction of theta and alpha travelling waves modulates human memory processing. Nat. Hum. Behav. 8, 1124–1135. https://doi.org/10.1038/s41562-024-01838-3.

Pang, Z., Alamia, A., VanRullen, R., 2020. Turning the stimulus on and off changes the direction of α traveling waves. eNeuro 7. https://doi.org/10.1523/ENEURO.0218-20.2020. ENEURO.0218-20.2020.

Phookan, S., Sutton, A.C., Walling, I., Smith, A., O'Connor, K.A., Campbell, J.C., Calos, M., Yu, W., Pilitsis, J.G., Brotchie, J.M., Shin, D.S., 2015. Gap junction blockers attenuate beta oscillations and improve forelimb function in hemiparkinsonian rats. Exp. Neurol. 265, 160–170. https://doi.org/10.1016/j.expneurol.2015.01.004.

Rigotti, M., Barak, O., Warden, M.R., Wang, X.-J., Daw, N.D., Miller, E.K., Fusi, S., 2013. The importance of mixed selectivity in complex cognitive tasks. Nature 497, 585–590. https://doi.org/10.1038/nature12160.

Roopun, A.K., Middleton, S.J., Cunningham, M.O., LeBeau, F.E.N., Bibbig, A., Whittington, M.A., Traub, R.D., 2006. A beta2-frequency (20-30 Hz) oscillation in nonsynaptic networks of somatosensory cortex. Proc. Natl. Acad. Sci. 103, 15646–15650. https://doi.org/10.1073/pnas.0607443103.

Rubino, D., Robbins, K.A., Hatsopoulos, N.G., 2006. Propagating waves mediate information transfer in the motor cortex. Nat. Neurosci. 9, 1549–1557. https://doi.org/10.1038/nn1802.

Salkoff, D.B., Zagha, E., McCarthy, E., McCormick, D.A., 2020. Movement and performance explain widespread cortical activity in a visual detection task. Cerebral Cortex 30, 421–437. https://doi.org/10.1093/cercor/bhz206.

Samara, A., Eilbott, J., Margulies, D.S., Xu, T., Vanderwal, T., 2023. Cortical gradients during naturalistic processing are hierarchical and modality-specific. NeuroImage 271, 120023. https://doi.org/10.1016/j.neuroimage.2023.120023.

Sihn, D., Kim, J.S., Kwon, O.-S., Kim, S.-P., 2023. Breakdown of long-range spatial correlations of infraslow amplitude fluctuations of EEG oscillations in patients with current and past major depressive disorder. Front Psychiatry 14, 1132996. https://doi.org/10.3389/fpsyt.2023.1132996.

Sihn, D., Kim, S.-P., 2024. Disruption of alpha oscillation propagation in patients with schizophrenia. Clin. Neurophysiol. 162, 262–270. https://doi.org/10.1016/j.clinph.2024.02.028.

Soni, S., Muthukrishnan, S.P., Samanchi, R., Sood, M., Kaur, S., Sharma, R., 2019. Pre-trial and pre-response EEG microstates in schizophrenia: an endophenotypic marker. Behav. Brain Res. 371, 111964. https://doi.org/10.1016/j.bbr.2019.111964.

Staudigl, T., Minxha, J., Mamelak, A.N., Gothard, K.M., Rutishauser, U., 2022. Saccade-related neural communication in the human medial temporal lobe is modulated by the social relevance of stimuli. Sci. Adv. 8, eabl6037. https://doi.org/10.1126/sciadv.abl6037.

Steinmetz, N.A., Zatka-Haas, P., Carandini, M., Harris, K.D., 2019. Distributed coding of choice, action and engagement across the mouse brain. Nature 576, 266–273. https://doi.org/10.1038/s41586-019-1787-x.

Stolk, A., Brinkman, L., Vansteensel, M.J., Aarnoutse, E., Leijten, F.S.S., Dijkerman, C.H., Knight, R.T., de Lange, F.P., Toni, I., 2019. Electrocorticographic dissociation of alpha and beta rhythmic activity in the human sensorimotor system. eLife 8, e48065. https://doi.org/10.7554/eLife.48065.

Stringer, C., Pachitariu, M., Steinmetz, N., Reddy, C.B., Carandini, M., Harris, K.D., 2019. Spontaneous behaviors drive multidimensional, brainwide activity. Science 364, eaav7893. https://doi.org/10.1126/science.aav7893.

Szabadics, J., Lorincz, A., Tamás, G., 2001. β and γ frequency synchronization by dendritic GABAergic synapses and gap junctions in a network of cortical interneurons. J. Neurosci. 21, 5824–5831. https://doi.org/10.1523/JNEUROSCI.21-15-05824.2001.

Tarailis, P., Koenig, T., Michel, C.M., Griškova-Bulanova, I., 2024. The functional aspects of resting EEG microstates: a systematic review. Brain Topogr. 37, 181–217. https://doi.org/10.1007/s10548-023-00958-9.

Tenke, C.E., Kayser, J., Manna, C.G., Fekri, S., Kroppmann, C.J., Schaller, J.D., Alschuler, D.M., Stewart, J.W., McGrath, P.J., Bruder, G.E., 2011. Current source density measures of electroencephalographic alpha predict antidepressant treatment response. Biol. Psychiatry 70, 388–394. https://doi.org/10.1016/j.biopsych.2011.02.016.

Vinck, M., Uran, C., Spyropoulos, G., Onorato, I., Broggini, A.C., Schneider, M., Canales-Johnson, A., 2023. Principles of large-scale neural interactions. Neuron 111, 987–1002. https://doi.org/10.1016/j.neuron.2023.03.015.

von Wegner, F., Wiemers, M., Hermann, G., Tödt, I., Tagliazucchi, E., Laufs, H., 2024. Complexity measures for EEG microstate sequences: concepts and algorithms. Brain Topogr. 37, 296–311. https://doi.org/10.1007/s10548-023-01006-2.

Wang, X.-J., 2022. Theory of the multiregional neocortex: large-scale neural dynamics and distributed cognition. Annu. Rev. Neurosci. 45, 533–560. https://doi.org/10.1146/annurev-neuro-110920-035434.

Wang, J., Guo, M., Zhang, J., Bai, Y., Ni, G., 2025. Early audiovisual integration in target processing under continuous noise: behavioral and EEG evidence. Neuropsychologia 211, 109128. https://doi.org/10.1016/j.neuropsychologia.2025.109128.

Wang, X.-J., Yang, G.R., 2018. A disinhibitory circuit motif and flexible information routing in the brain. Curr. Opin. Neurobiol. 49, 75–83. https://doi.org/10.1016/j.conb.2018.01.002.

Westlin, C., Theriault, J.E., Katsumi, Y., Nieto-Castanon, A., Kucyi, A., Ruf, S.F., Brown, S.M., Pavel, M., Erdogmus, D., Brooks, D.H., Quigley, K.S., Whitfield-Gabrieli, S., Barrett, L.F., 2023. Improving the study of brain-behavior relationships by revisiting basic assumptions. Trends on Cognitive Sci. 27, 246–257. https://doi.org/10.1016/j.tics.2022.12.015.

Yu, H., Lei, X., Song, Z., Liu, C., Wang, J., 2020. Supervised network-based fuzzy learning of EEG signals for alzheimer's disease identification. IEEE Trans. Fuzzy Syst. 28, 60–71. https://doi.org/10.1109/TFUZZ.2019.2903753.

Yu, H., Li, F., Liu, J., Liu, D., Guo, H., Wang, J., Li, G., 2024. Evaluation of acupuncture efficacy in modulating brain activity with periodic-aperiodic EEG measurements. IEEE Trans. Neural Syst. Rehabil. Eng. 32, 2450–2459. https://doi.org/10.1109/TNSRE.2024.3421648.

Yu, H., Wu, X., Cai, L., Deng, B., Wang, J., 2018. Modulation of spectral power and functional connectivity in human brain by acupuncture stimulation. IEEE Trans. Neural Syst. Rehabil. Eng. 26, 977–986. https://doi.org/10.1109/TNSRE.2018.2828143.

Yu, H., Zeng, F., Liu, D., Wang, J., Liu, J., 2025. Neural manifold decoder for acupuncture stimulations with representation learning: an acupuncture-brain interface. IEEE J. Biomed Health Inform 29, 4147–4160. https://doi.org/10.1109/JBHI.2025.3530922.

Zabeh, E., Foley, N.C., Jacobs, J., Gottlieb, J.P., 2023. Beta traveling waves in monkey frontal and parietal areas encode recent reward history. Nat. Commun. 14, 5428. https://doi.org/10.1038/s41467-023-41125-9.

Zappasodi, F., Perrucci, M.G., Saggino, A., Croce, P., Mercuri, P., Romanelli, R., Colom, R., Ebisch, S.J.H., 2019. EEG microstates distinguish between cognitive components of fluid reasoning. NeuroImage 189, 560–573. https://doi.org/10.1016/j.neuroimage.2019.01.067.

Zhang, H., Watrous, A.J., Patel, A., Jacobs, J., 2018. Theta and alpha oscillations are traveling waves in the human neocortex. Neuron 98, 1269–1281. https://doi.org/10.1016/j.neuron.2018.05.019. .e4.